The Effect of Span-to-depth Ratio on the Flexural Properties of Hybrid S2/E-Glass Fiber-reinforced Epoxy Composites

Sudarisman

Department of Mechanical Engineering, Universitas Muhammadiyah Yogyakarta, Jl. Lingkar Barat, Tamantirto, Kasihan, Yogyakarta 55183, INDONESIA

E-mail: sudarisman@umy.ac.id, sudarisman05@yahoo.com.au

Abstract

High strength synthetic fiber-reinforced polymer composite beams are commonly failed by kinking at their compressive faces. Partial replacement of the fibers at the weaker faces with stronger fibers to produced hybrid fiber composite systems can improved their performance. In addition, their applied shear-to-normal stress ratio can affect their The effect of span-to-depth ratio, *S*/*d*, on the flexural properties of hybrid S2/E-fiber-reinforced epoxy composites has been investigated. *S*/*d* of 16, 32 and 64 have been selected, and six plates of different hybrid ratios, *i.e.* 0.0, 0.2, 0.4, 0.6, 0.8 and 1.0, have been fabricated using compression molding technique in vacuum environment. Before being stacked depending upon the hybrid ratio and pressed in the mold, the fibers were embedded into the matrix to produce glass/epoxy prepreg sheets possessing a thickness of ~0.45 mm. The thickness of the plates being produced is ~2 mm. Flexural test was carried out in accordance with the ASTM D790 in an Instron Universal Testing Machine at room temperature and applying strain rate of ~1 percent/minute. Five specimens have been tested for each case as recommended by the standard. The specimens were cut from the plates using a diamond-tipped circular saw blade rotating at ~10,000 rpm. A number of failed specimens from the flexural test were randomly selected to be prepared for micrograph capturing under an optical microscope. It was reveals that the larger the *S*/*d* the higher flexural strength and flexural modulus. To the contrary, slight decrease in flexural failure strain was noted with the increase of *S*/*d*. All specimens were found to fail at their compressive sides by fiber and matrix crushing. At *S*/*d* =16, fail was initiated with longitudinal cracks followed by fiber and matrix crushing, but longitudinal crack was not observed for longer beams.

Keywords: hybrid GFRP composite, span-to-depth ratio, hybrid ratio, flexural strength, flexural modulus, flexural strain-to-failure.

Introduction

Being known for their superior properties compared to conventional materials has led to wide acceptance of composite materials ranging from household appliances to high performance structures. Among their advantages is that they can be designed and fabricated according to their respective applications and required properties, either by selecting the matrix and reinforcing materials, controlling fiber-matrix proportions, fiber architecture, or any combinations of them.

Composite materials containing mixed fiber in a common matrix has been studied and reported. Various combinations of fibers have been investigated, such as: glass and carbon fibers [1-2], glass and graphite fibers [3-4], glass and steel fibers [5], carbon and aramid fibers [6], glass and aramid fibers [7], carbon and silicon carbide fibers [8], sisal and aramid fibers [9], as well as glass and bamboo fibers [10]. However, very limited number and very difficult to find published report on improving the mechanical properties of low cost E-glass FRP composites by partial replacement of superior mechanical property S2-glass fiber to produce hybrid glass FRP composites.

The current work has been focused on the effect of span-to-depth ratio on the flexural properties, *i.e*. flexural strength, flexural strain and flexural modulus and work of fracture, of hybrid E/S2-glass FRP composite by partial substitution of up to ~80% of S2-glass for E-glass fiber in the compressive side of the beams.

Research Method

SE 2350 type 30® single-end continuous glass fiber roving produced by Owens Corning, Tokyo, Japan, and unidirectional plain wave UT-S500 S2-glass® fiber produced by AGY Europe, 163 Bld des Etats Unis, Lyon, France, have been used for reinforcement in this work. Their properties have been presented in Table 1. The matrix being used is Kinetix® R104 epoxy resin combined with Kinetix® H125 hardener. The

Table 1. Fiber Properties

Type	Density, ρ (g/cm^3)	Tensile strength, σ_f (MPa)	Tesile modulus, E (GPa)
E [11]	2.58	2240	72.3
S2 (23 ^{o}C) [12]	2.46	4890	86.9

mixing ratio being recommended by the manufacturer was 100 to 43 by weight. Matrix density calculated according to the rule of mixtures using the data obtained from the supplier was 1.09 g/cm^3. Unidirectional glass fiber-epoxy matrix prepreg sheets were first prepared by winding the glass fiber tows or mats onto a steel rectangular frame and wetting the fibers in epoxy system solution in acetone containing 50 vol% of epoxy system. Excess resin solution was let to drain from the wet glass fibers then followed by a partial curing procedure carried out in an oven with heating rate of ~10 ^{o}C·min^{-1} and held at 120 ^{o}C for 12 minutes. After being cut into sections of ~150 mm × ~290 mm, the glass fiber-epoxy prepreg was then stacked into a five-layer unidirectional plate. The resulting prepreg plates were cured under ~0.35 MPa vacuum pressure and ~1 MPa compressive pressure in an autoclave at ~120 ^{o}C and 30 minutes holding time. The thickness of the resulting plates was varied from 4.06 mm to 4.92 mm.

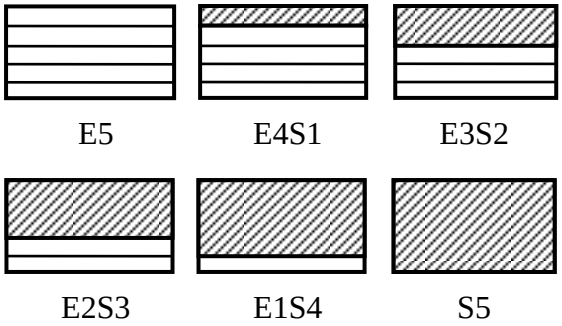

Figure 1. Stacking configurations

Six different stacking configurations (Figure 1), namely E5, E4S1, E3S2, E2S3, E1S4 and S5 designated for plates as illustrated in Figure 1, have been fabricated. The tests were carried out in accordance with the ASTM D790 standard [13]. Specimens were cut from each composite plate using a diamond-tipped circular saw blade rotating at ~6000 rpm with the resulting specimen width of approximately 12.7 mm and length according to their respective span-to-depth ratios.

Flexural testing using the 3-point bending was carried out in a universal testing machine equipped with an adjustable-span flexural test fixture. Procedure A of the adopted test standard was implemented, and three different span-to-depth ratios of 16, 32 and 64 were utilized. The crosshead speed was set being equivalent to a strain rate of 1% min^{-1} as recommended by the testing procedure.

All presented data being presented are the average of at least five tests for each case. According to the ASTM D790 standard, the magnitude of modulus, E_f, flexural strength, σ_f, and flexural strain, ε_f, were calculated according to the adopted standard using equations (1) – (3).

$$\sigma_f = \begin{cases} \dfrac{3FS}{2wd^2}; & \dfrac{S}{d} \le 16 \quad (1a) \\ \dfrac{3FS}{2wd^2}\left[1+\dfrac{6D^2}{S^2}-\dfrac{4Dd}{S^2}\right]; & \dfrac{S}{d} > 16 \quad (1b) \end{cases}$$

$$\varepsilon_f = \frac{6\,Dd}{S^2} \quad (2)$$

and

$$E_f = \frac{S^3}{4\,bd^2}\cdot\frac{\Delta F}{\Delta D} \quad (3)$$

where F is the magnitude of the maximum load (N), S is the span (mm), b is the specimen width (mm), d is the specimen depth (mm), D is the vertical deflection of the specimen centerline (mm), and $\Delta F/\Delta D$ is the slope of the linear region of the force-displacement curve ($N \cdot m^{-1}$).

Result and Dicussion

Flexural Strength. Figure 2 shows the effect of *S*/*d* on flexural strength for various hybrid ratios. Apart from the increase of span-to-depth ratio, *S*/*d*, from 32 to 64 for r_h = 0.4 and r_h = 0.6 specimens, generally speaking, it shows that flexural strength increases with the increase of *S*/*d*. Larger increase of flexural strength was found when *S*/*d* was increased from 16 to 32 in comparison with that of S/d increase from 32 to 64. The change of failure mode from longitudinal cracking for *S*/*d* = 16 specimens (Figure 6(a)) due to higher shear-to-normal stress ratio at mid-span cross section into fiber and matrix crushing for *S*/*d* = 32 and *S*/*d* = 64 (Figure 6(b) and (c)) due to lower shear-to-normal stress ratio at mid-span may be responsible for such increase, as has been pointed out by Davies and Hamada [14]. When *S*/*d* was increases from 16 to 32, the highest increase (~31.6%) from ~650 MPa to ~855 MPa was obtained for r_h = 0.6, and the lowest increase (~18.8%) from ~596 MPa to ~708 MPa was obtained for r_h = 0, *i.e*. E-glass/epoxy composites. When *S*/*d* was increases from 32 to 64 the increase of flexural strength was found considerably insignificant, ranging from ~–1.7% (decrease) for r_h = 0.6 to ~2.8% for r_h = 1.0, *i.e*. S2-glass/epoxy composites.

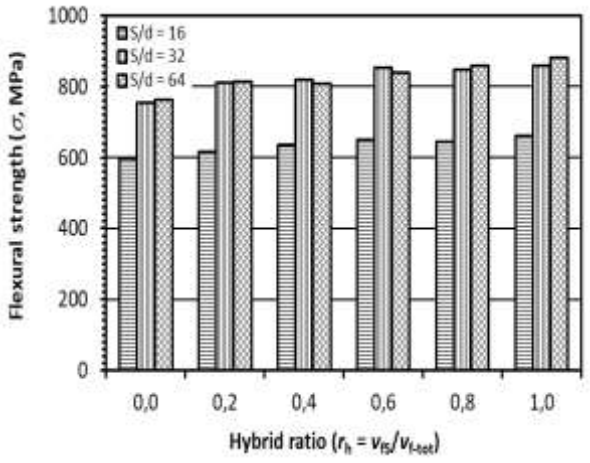

Figure 2. The effect of *S*/*d* on the flexural strength

In addition, for all the three *S*/*d*, there is a slight increase of flexural strength with partial substitution of S2-glass fiber to produce hybrid GFRP composite specimens. Considering the mechanical properties of the fibers as presented in Table 1, this increase seems to obey the rule of mixtures.

Flexural Failure Strain. The effect of *S*/*d* on flexural failure strain for various hybrid ratios has been presented in Figure 2. Flexural failure strain tends to increase with the increase of *S*/*d*, except for r_h = 0.2 specimens. The highest failure strain was found being 2.91% for *S*/*d* = 16 and rh = r_h = 0.2, and the lowest is 1.67% for *S*/*d* = 16 and r_h = 0.8. At

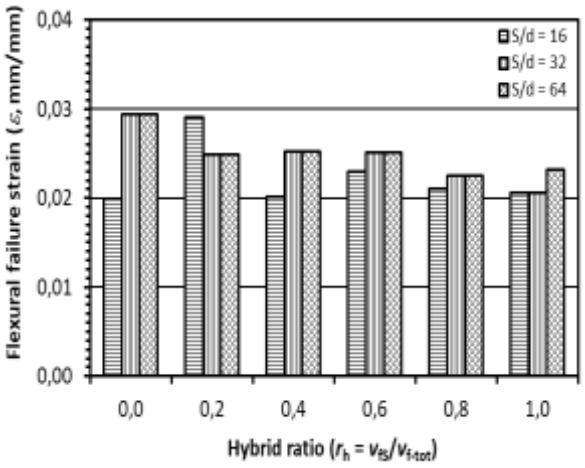

Figure 3. The effect of *S*/*d* on the flexural strain

higher *S*/*d*, failure strains were found to vary between 2.08 % for *S*/*d* = 32 and r_h = 1, *i.e.* S2-glass/epoxy composite, and 2.86 % for *S*/*d* = 64 and r_h = 0, *i.e.* E-glass/epoxy composite. Thus, for longer beams, S/d > 16, strain-to-failure of the hybrid systems was found between that of the E-glass/epoxy composite and that of the S2-glass/epoxy composites.

Partial replacement of E-glass fiber with S2-glass fiber on the compressive side of the beams resulted in the slight decrease of flexural failure strain, especially for *S*/*d* = 32 and *S*/*d* = 64. E-glass/epoxy specimens exhibits the highest failure strain for both *S*/*d* = 32 and *S*/*d* = 64.

Flexural Modulus. Similar to that observed for flexural strength, Figure 4 shows that there is an increase in flexural modulus with the of *S*/*d*, and the magnitude of increase from that of *S*/*d* = 16 to that of *S*/*d* = 32 was significantly larger than that of *S*/*d* = 32 to *S*/*d* = 64. When s/d was increased from 16 to 32, the increase of flexural modulus was found varies from 5.75 % for E-glass/epoxy composite to 11.48 % for S2-glass/epoxy composites, while those of the hybrid system were found being between these two values. The lowest flexural modulus, E_f, was found being 31.60 GPa for *S*/*d* = 16 and r_h = 0, and the highest was found being 40.98 GPa for *S*/*d* = 64 and r_h = 1. Similar to their respective flexural strengths, flexural modulus for *S*/*d* = 16 is considerably lower than those of the other two S/d values, while those of *S*/*d* = 32 and *S*/*d* = 64 are very close to each other. This finding is closely in line with those previously reported by Davies and Hamada [14] for C/SiC hybrid FRP composite where they observed that flexural modulus of *S*/*d* = 16 specimens was significantly lower, while those of *S*/*d* = 32 and *S*/*d* = 64 were very close to each other.

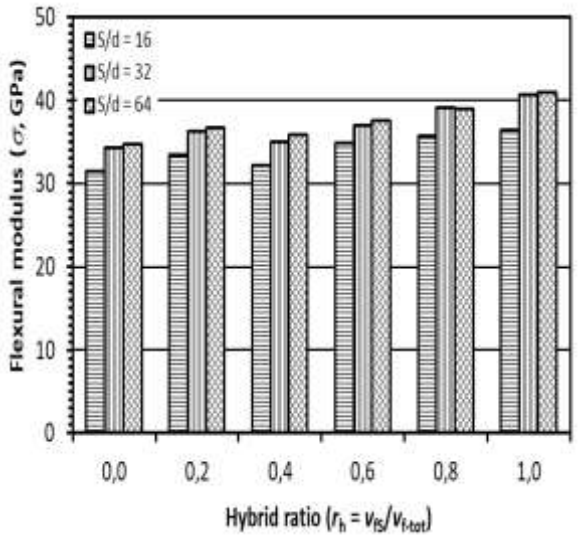

Figure 4. The effect of *S*/*d* on the flexural modulus

Considering the modulus of the fibers as given in Table 1, these values were slightly lower than those predicted by the rule of mixtures. This negative deviation may be attributed to the imperfect structural integrity of the composite as can be observed in Fig 5(a). In addition, for all the three *S*/*d* values, flexural modulus was observed tending to increase with the increase S2-glass fiber content partially substituting the existing E-glass fiber to produce hybrid GFRP composite specimens.

Failure Modes. Fiber distribution within the matrix, and flexural failure modes of the three different *S*/*d* values has been depicted in Figure 5 and Figure 6, respectively.

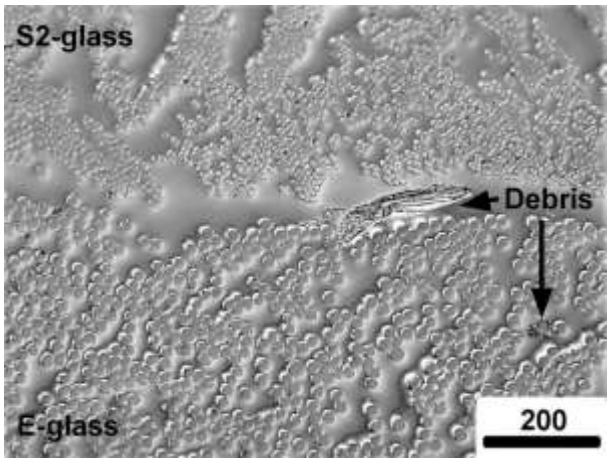

Figure 5. Fiber distributions

In can be seen in Figure 5 that the E-glass fibers are more evenly distributed in comparison with the S2-glass fibers. Larger and more matrix-rich areas can be seen in the S2-glass/epoxy layer. Such uneven S2-glass fiber distribution can be caused by the fully manual fiber lay-up where its parameter cannot be precisely controlled. Some debris

that may decrease its mechanical properties can also be observed.

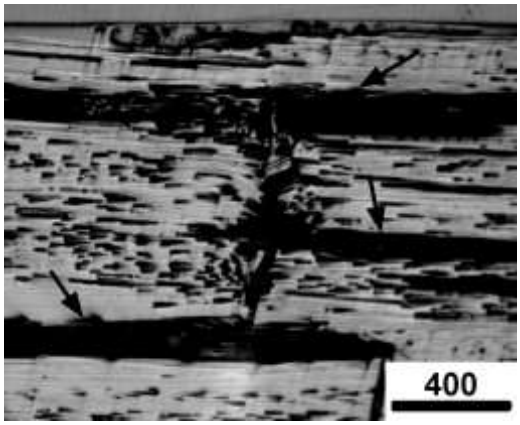

(a) *S*/*d* = 16

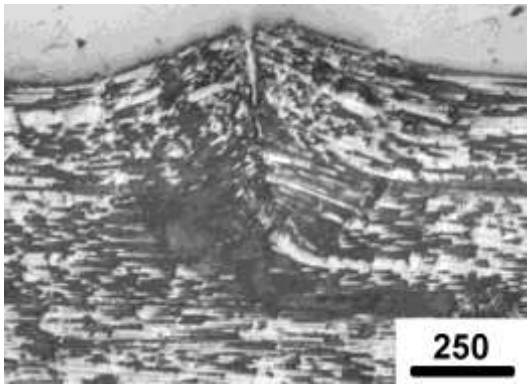

(b) *S*/*d* = 32

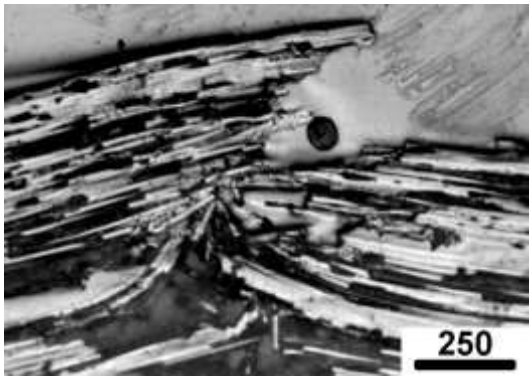

(c) *S*/*d* = 64

Figure 6. Failure modes found at compressive sides of the beams

Longitudinal cracks (dark-color arrows) that may be caused by high shear-to-normal stress ratio can be observed for shorter beams in Figure 6(a). After the formation of longitudinal crack, the cross-sectional second moment of inertia would be lower causing generation of higher normal stress at the same magnitude of lateral loading, leading to earlier failure. Unlike Figure 6(a), longitudinal crack cannot be seen in Figures 6(b) and (c). It indicates that failure in this area is fiber and matrix crushing due to higher shear-to-normal stress ratio. Higher magnification images, not presented here, shows that out of plane fiber microbuckling and kink band formation due mainly to fiber misalignment took place, as has been reported for GFRP composites by Barulich et al, prior to crushing.

Conclusion

It can be concluded that larger *S*/*d* resulted in higher flexural strength and flexural modulus. Slight decrease in flexural failure strain was noted with the increase of *S*/*d*. All specimens were found to fail at their compressive sides by fiber and matrix crushing. At *S*/*d* =16, fail was initiated with longitudinal cracks followed by fiber and matrix crushing, but longitudinal crack was not observed for longer beams.

References

[1] C.S. Dong, Sudarisman, I.J. Davies, Flexural Properties of E Glass and TR50S Carbon Fiber Reinforced Epoxy Hybrid Composites, J. Mater Eng Perf 22(1) (2013) 41-49.

[2] G. Belingardi, M.P. Cavatorta, C. Frasca, Bending fatigue behavior of glass–carbon/epoxy hybrid composites, Compos Sci Tech 66 (2006) 222-232.

[3] S.S. Daryadel, C. Ray, T. Pandya, P.R. Mantena, Energy Absorption of Pultruded Hybrid Glass/Graphite Epoxy Composites under High Strain-Rate SHPB Compression Loading, Mater Sci App 6 (2015) 511-518.

[4] M.N. Ahmed, P.V. Kumar, H.K. Shivanand, S.B. Muzammil, A study on flexural strength of hybrid polymer composite materials (E-glass fibre-carbon fibre-graphite) on different matrix material by varying its thickness, I.J. Mech Eng Tech 4(4) (2013) 274-286.

[5] A. McBride, Mechanical Behavior of Hybrid Glass/Steel Reinforced Epoxy

Composites, Master's Theses (2016) Univ Connecticut.

[6] L.X. Zhong, S.Y. Fu, X.S. Zhou, H.Y. Zhan, Effect of surface microfibrillation of sisal fiber on the mechanical properties of sisal/aramid fiber hybrid composites, Compos Part A 42 (2011) 244–252.

[7] N. Shaari, A. Jumahata, M.K.M. Razif, Impact resistance propertyies of Kevlar/glass fiber hybrid composite laminates, Jurnal Teknologi 76(3) (2015) 93–99.

[8] Sudarisman, Davies, I.J. and Hamada, H., Compressive failure of unidirectional hybrid fibre-reinforced epoxy composites containing carbon and silicon carbide fibres, Compos Part A 38(3) (2007) 1070-1074.

[9] Y. Li, X.J. Xian, C.L. Choy, M.Guo, Z. Zhang, Effect of surface microfibrillation of sisal fiber on the mechanical properties of sisal/aramid fiber hybrid composites, Compos Sci Tech 59, 1999, pp. 13-18.

[10] M.M. Thwe, K. Liao, Durability of bamboo-glass fiber reinforced polymer matrix hybrid composites, Compos Sci Tech 63 (2003) 375-387.

[11] Owen Cornings, OC® SE 2350 Single-end Continuous Rovings (TYPE 30®), Prod Info, 2014.

[12] AGY Europa, high strength glass fibers Lyon, France (2004).

[13] Ann Book of ASTM Standards, Vol 08.01, ASTM, 2005, pp. 149-159.

[14] I.J. Davies, H. Hamada, Flexural properties of a hybrid polymer matrix composite containing carbon and silicon carbide fibres, Adv Compos Mater 10(1) (2001) 77-96.

[15] N.D. Barulich, L.A. Godoy, E.J. Barbero, On micro-buckling of unidirectional fiber-reinforced composites by means of computational micromechanics, Lat Amer J Sol and Struct 13 (2016) 3085-3106.